Journal of Biomedical Optics

SPIEDigitalLibrary.org/jbo

In vivo fluorescence lifetime detection of an activatable probe in infarcted myocardium

Craig J. Goergen
Howard H. Chen
Alexei Bogdanov, Jr.
David E. Sosnovik
Anand T. N. Kumar

SPIE

In vivo fluorescence lifetime detection of an activatable probe in infarcted myocardium

Craig J. Goergen,[a] Howard H. Chen,[b] Alexei Bogdanov Jr.,[c] David E. Sosnovik,[d,*] and Anand T. N. Kumar[a,*]
[a]Harvard Medical School, Athinoula A. Martinos Center for Biomedical Imaging, Massachusetts General Hospital, Charlestown, Massachusetts 02129
[b]Harvard Medical School, Center for Molecular Imaging Research, Massachusetts General Hospital, Charlestown, Massachusetts 02129
[c]University of Massachusetts Medical School, Laboratory of Molecular Imaging Probes, Department of Radiology, 55 Lake Avenue North, Worcester, Massachusetts 01605
[d]Harvard Medical School, Athinoula A Martinos Center for Biomedical Imaging and Center for Molecular Imaging Research, Massachusetts General Hospital, Charlestown, Massachusetts 02129

Abstract. Activatable fluorescent molecular probes are predominantly nonfluorescent in their inactivated state due to intramolecular quenching, but increase fluorescence yield significantly after enzyme-mediated hydrolysis of peptides. Continuous wave *in vivo* detection of these protease-activatable fluorophores in the heart, however, is limited by the inability to differentiate between activated and nonactivated fractions of the probe and is frequently complicated by large background signal from probe accumulation in the liver. Using a cathepsin-activatable near-infrared probe (PGC-800), we demonstrate here that fluorescence lifetime (FL) significantly increases in infarcted murine myocardial tissue (0.67 ns) when compared with healthy myocardium (0.59 ns) after 24 h. Furthermore, we show that lifetime contrast can be used to distinguish *in vivo* cardiac fluorescence from background nonspecific liver signal. The results of this study show that lifetime contrast is a helpful addition to preclinical imaging of activatable fluorophores in the myocardium by reporting molecular activity *in vivo* due to changes in intramolecular quenching. This characterization of FL from activatable molecular probes will be helpful for advancing *in vivo* imaging of enzyme activity. [DOI: 10.1117/1.JBO.17.5.056001]

Keywords: near-infrared fluorescence; lifetime; myocardium; protease.

Paper 12016 received Jan. 6, 2012; revised manuscript received Mar. 2, 2012; accepted for publication Mar. 5, 2012; published online Apr. 20, 2012.

1 Introduction

Fluorescence imaging of mice has many advantages over techniques such as magnetic resonance imaging (MRI) and positron emission tomography (PET).[1] Fluorescence imaging is rapid, high-throughput, and does not involve ionizing radiation.[2] In addition, fluorescence imaging is ideally suited for the imaging of enzyme-activatable fluorophore-labeled probes, such as those activated by proteases.[3] Traditional continuous wave (CW) fluorescence excitation techniques have been used to image cyanine fluorophores in the heart.[4,5] A drawback in CW imaging is the inability to separate probe concentration from lifetime, since both the amount of probe and lifetime of the fluorophore signal independently contribute the measured CW intensity.[6] When imaging activatable probes where nonradiative quenching could be an underlying mechanism, this implies an inability to separate the contribution of probe uptake (concentration) from that of probe activation (lifetime) to the total fluorescence intensity.[6] In addition, the inactivated fluorophore-labeled probe is usually not completely optically silent (i.e., 100% quenched). If both unactivated and activated states have distinct lifetimes and contribute to overall fluorescence intensity, then lifetime imaging would be needed to decouple these factors. When injected *in vivo*, probe activation (and hence an increase in intensity) can also occur due to enzyme cleavage within internal organs such as the liver.[7] These effects result in significant background (or nonspecific) fluorescent signal. Given the limited spatial resolution and diffuse nature of fluorescence imaging, the large background from both the inactivated probe and the probe accumulation in the liver can significantly compromise the accuracy of fluorescence imaging in the heart.[4]

While fluorescence CW intensity reflects both probe concentration and lifetime, time domain (TD) fluorescence can separate the two quantities and allow an improved localization of multiple lifetime components *in vivo*.[8] Previous applications of TD lifetime imaging have largely been restricted to microscopy techniques.[9] Whole-body TD molecular imaging of lifetime contrast is, however, relatively recent.[10–15] The use of fluorescence lifetime (FL) as a contrast mechanism may be particularly relevant to activatable probe measurements, where fluorescence lifetime (FL) could serve as a functional reporter of probe environment independent of fluorophore concentration.[16] While lifetime-based whole-body imaging of targeted [13,14,17] and intrinsic[18] fluorescence has already been reported, lifetime imaging has not been previously employed to image activatable probes in the heart.

Whole-body small animal imaging with protease-activatable probes has previously been performed with CW detection from a steady state, or nonpulsed, light source.[7] Originally developed for tumor imaging,[19] these probes are composed of a long-circulating copolymer backbone with self-quenched fluorophores in the inactive state.[20] Activation of these probes can be specific for a single enzyme, such as cathepsin-D,[21] or a group of enzymes, such as matrix metalloproteinases.[22] These studies demonstrate that near-infrared fluorescence (NIRF) is generated when lysosomal proteases cleave the probe, releasing

*These authors contributed equally to this work.

Address all correspondence to: Anand T. N. Kumar, Harvard Medical School, Athinoula A. Martinos Center for Biomedical Imaging, Massachusetts General Hospital, Charlestown, Massachusetts 02129. Tel: +617 7268394; E-mail: ankumar@nmr.mgh.harvard.edu

0091-3286/2012/$25.00

previously quenched fluorochromes.[7] Others using models of ischemic myocardial injury in mice[4] have shown that infiltration of inflammatory cells into injured areas generates large amounts of proteases and a significant increase in fluorescent signal in both *in vivo* and *ex-vivo* images.[5] This leukocyte infiltration occurs within 24 to 48 h of injury and persists for up to 10 days, generating large amounts of proteases, such as cathepsins, which can be detected with cathepsin-activatable near-infrared fluorochromes.

We hypothesized that 1) cleavage would increase the FL of a cathepsin-activatable molecular probe and 2) there would be significant variation in probe lifetime between the liver and infarcted myocardium. In order to test these, we performed TD fluorescence measurements of probe lifetime *in vitro* after activation with cathepsin and *in vivo* in mice post-coronary ligation. The purpose of this study was to determine if TD measurements with lifetime-sensitive detection could be used to improve *in vivo* imaging of protease activation in inflamed cardiac tissue, with the hope of aiding in the detection and characterization of myocardial infarctions.

2 Methods

2.1 *Probe Synthesis and Trypsin Activation*

The macromolecular probe, a graft copolymer of poly-l-lysine and methoxy polyethylene glycol, was prepared as described in reference[20,21,23,24,] with some modifications. Briefly, PGC [a graft copolymer backbone of O-methoxypoly(ethylene glycol)-]O′-succinate with a m.w. ~5 kD and poly-l-lysine (degree of polymerization: 225, mass = 52700 by viscosity; Mw/Mn = 1.15, 25% amino groups grafted with MPEG-succinate) was dissolved at the concentration of 10 mg/ml 0.1 M sodium bicarbonate (pH 8.5) and stored frozen in aliquots. To synthesize the probe, 800CW hydoxysuccinimide ester (800CW-HSE, catalog number 929 to 70020, Li-COR) was dissolved at 25 mg/ml (21.4 mM) in dry DMSO. A 2.8 μl aliquot of 800CW-HSE was added to 50 μl of PGC solution (PGC concentration 32 μM) while mixing with a Vortex and kept in the dark for 3 h. The final ratio was 14 mol 800 CW/mol PGC. The conjugate was purified by performing two consecutive spin-centrifugations using Bio-Spin P30 microcolumns (catalog number 732 to 6006, Bio-Rad) equilibrated with 1xSSC. The 800CW dye coupling efficiency to PGC was 98%. Activation of the probe by pancreatic trypsin (a model serine protease) was achieved by incubating the synthesized macromolecular probe, PGC-800, at 13 μM of 800CW in PBS in the presence of 0.3 mg/ml trypsin for 2 h at room temperature.

2.2 *Animal Model*

All procedures were performed with local Institutional Animal Care and Use Committee approval. The C57BL/6 mice used in this study were between eight and 12 weeks old and anesthetized with 1 to 3% isoflurane in 2 L/ min O_2 during the surgical and *in vivo* imaging procedures. We used a murine left coronary artery permanent occlusion model to determine if FL changes would be present *in vivo*.[25] With this model, inflammatory cells are recruited into the ischemic area and contribute to the remodeling of the left ventricle through production and activation of a wide variety of proteases.[5] A total of six mice underwent ligation surgery and received a dose of PGC-800 (2 nmol 800 CW/150 µL diluted in PBS via intravenous tail vein injection) 24 h before sacrifice. A second control group of three additional mice did not undergo surgery, but were dosed with PGC-800 at the same concentration.

2.3 *Fluorescence Lifetime Imaging System*

A detailed description of the TD imaging system used here has been described previously.[8] The primary excitation source was a Ti:Sapphire laser with a 100-fs pulse width, 40/80-MHz repetition rate, and 690 to 1020 nm tuning range (Mai Tai, Newport-Spectra Physics, Mountain View, CA). A gated intensified charge-coupled device (CCD) camera (Lavision, Goettingen, Germany) provided noncontact reflectance fluorescence detection with 200-ps time resolution. The light output from the Ti:Sapph was launched into a 200-μm core SMA connectorized fiber using a fiber collimation package. The light at the output end of the fiber was expanded to cover an area 2×2 cm^2. All imaging done in this study was with 750-nm excitation and 800-nm longpass emission. Anesthetized animals were placed in a supine position four to five days post surgery, with a large ventral region illuminated for reflectance TD imaging. Body temperature was maintained with a heating pad placed underneath each animal.

2.4 *Image Analysis*

Lifetime analysis was performed using both single and bi-exponential analysis. The single exponential analysis is performed by fitting the asymptotic portion of the TD data with a simple exponential:

$$U(\mathbf{r}, t) = a(\mathbf{r}) \exp[-t/\tau(\mathbf{r})], \tag{1}$$

where τ is the FL and $\mathbf{r}$ is the location of an image pixel.[8] Lifetime maps were created by calculating the fluorescent lifetime decay at each pixel. The single exponential is used for the *ex-vivo* images, where it can be assumed that each pixel is a mono-exponential. The single exponential analysis also used to obtain a visual representation of the mean surface lifetimes for the *in vivo* measurements.

The lifetimes obtained from single exponential analysis of the *ex-vivo* images of the dissected myocardium and liver are next used as *a priori* lifetimes in a linear bi-exponential fit to the following function:

$$U(\mathbf{r}, t) = a_{\text{th}}(\mathbf{r}) \exp(-t/\tau_{\text{th}}) + a_b(\mathbf{r}) \exp(-t/\tau_b), \tag{2}$$

where τ_{th} and τ_b are *a priori* lifetimes of the thoracic and background components, respectively. This "channel" analysis allows the separation of the thoracic and background components *in vivo*. Furthermore, the pixel-wise decay amplitudes a_{th} can subsequently be used in tomography algorithms to obtain quantitative three-dimensional (3-D) distributions of fluorescence from the thoracic region alone.[8]

2.5 *In Situ Imaging and Tissue Preparation*

After sacrifice, *in situ* fluorescence imaging with the removal of ventral skin, muscle, and ribs was performed. The hearts were dissected, sliced axially, and stained with 1% triphenyltetrazolium chloride (TTC) at room temperature for 20 to 25 min. The tissue was then washed in PBS and imaged with the TD system. Both infarcted and remote regions of interests were manually

defined with guidance from the TTC staining for each animal at one axial slice midway through the ventricle.

2.6 *Statistics*

Data are presented as mean ± SD, and statistical significance was determined with a student's *t*-test followed by a Bonferroni correction for multiple comparisons.

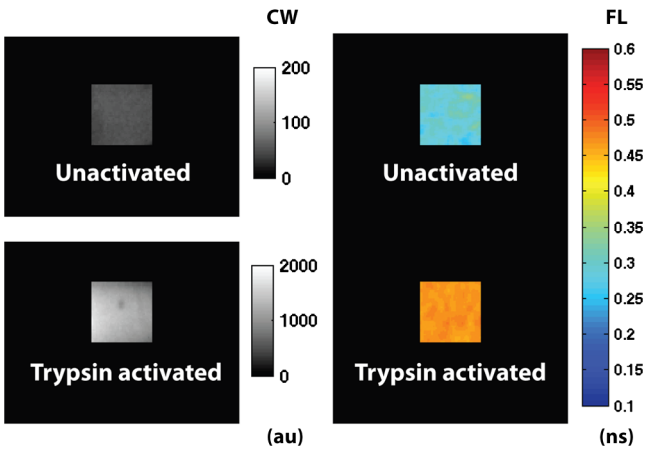

Fig. 1 PGC-800 continuous wave (CW) in grayscale and fluorescence lifetime (FL) time domain images in a pseudo-color scale before and after incubation with trypsin (13 μM of 800CW in PBS, 0.3 mg/ml trypsin, 2 h at room temperature). CW increased from 50 ± 4.7 arbitrary units (au) to 1185 ± 196 au after trypsin cleavage. FL also increased from the unactivated state (0.29 ± 0.01 ns) to the activated state (0.47 ± 0.01 ns).

3 Results

3.1 *Probe Activation Increases Lifetime in Vitro*

Both the CW intensity and FL increased substantially for PGC-800 after cleavage with pancreatic trypsin (Fig. 1). The CW intensity increased by over 20-fold after trypsin cleavage (from 50 ± 4.7 to 1185 ± 196 arbitrary units after activation), while the lifetime increased from 0.29 ± 0.01 ns to 0.47 ± 0.01 ns.

3.2 *Lifetime Contrast Improves Detection of Protease Activation in Vivo*

CW images from *in vivo* fluorescence measurements show a large signal in the hepatic region over the liver (Fig. 2). The corresponding lifetime images for the infarcted animal show significantly longer lifetimes in the thoracic region (0.70± 0.03 ns) than the hepatic (0.53 ± 0.04 ns; $p < 0.05$). The lifetime in the hepatic region of control animals was 0.48 ± 0.01 ns.

3.3 *Dual Lifetime "Channel" Analysis Separates Thoracic and Background Signal*

The dual "channel" analysis of the *in vivo* TD images (Fig. 3) was performed using Eq. (2), with the thoracic lifetime (τ_{th}) and background lifetime (τ_b) set to the values determined from *ex-vivo* heart and liver images ($\tau_{th} = 0.67$ ns; $\tau_b = 0.51$ ns; see Figs. 4, and 5). The thoracic and background amplitudes were merged into a single RGB image, with the amplitude of the thoracic channel (a_{th}) assigned to the red component and

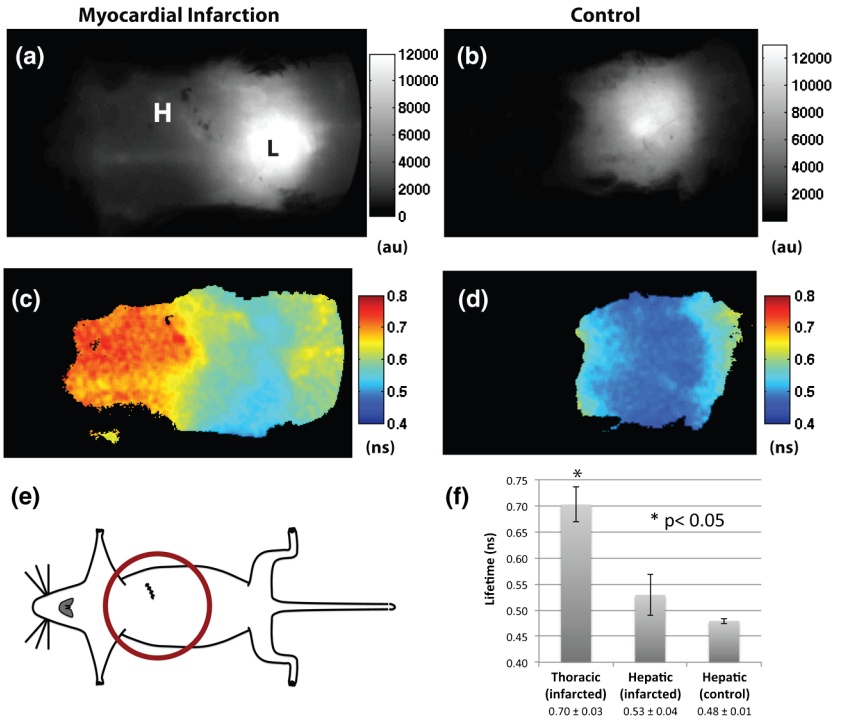

Fig. 2 Lifetime contrast improved *in vivo* detection of protease activation in infarcted myocardium. CW images of both infarcted (a) and control (b) animals showed a large signal from the liver (L), making signal from the heart (H) difficult to quantify. However, lifetimes from the heart and liver regions in the infarcted mouse (c) showed a 32% difference (0.70 ± 0.03 vs. 0.53 ± 0.04 ns). The control mouse (d) showed a more uniform lifetime near 0.48 ± 0.01 ns. The region imaged and location of the closing sutures are highlighted in the schematic (e). The increased lifetime in the thoracic region in animals undergoing coronary ligation (f) was significant compared to the hepatic region in both infarcted and control animals ($p < 0.05$).

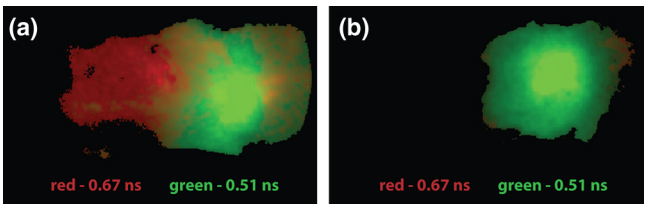

Fig. 3 Lifetime "channel" analysis using a bi-exponential fit with *a priori* lifetimes of 0.67 and 0.51 ns of both infarcted (a) and control (b) animals clearly delineated the thoracic (red—a_{th}) and background (green—a_b) regions.

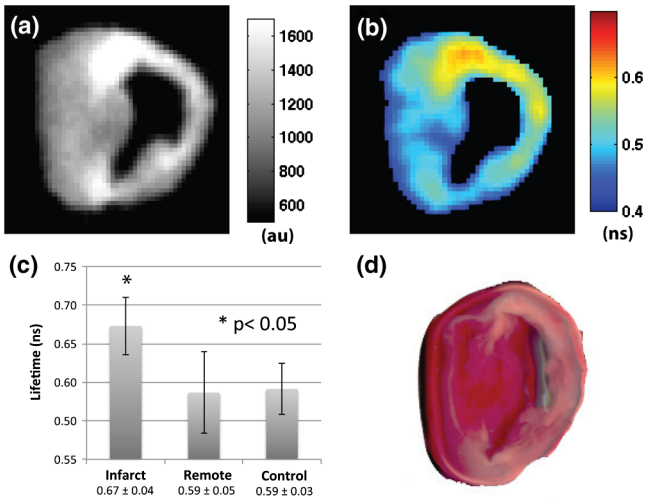

Fig. 4 Lifetime and probe concentration increased within ischemic areas of a myocardial infarction. CW (a) and lifetime images (b) of an axial slice from a mouse four days after coronary ligation and dosed with PGC-800 24 h before euthanasia. Probe accumulation was clearly seen in the area of ischemic injury and lifetime also increased within infarcted regions when compared to remote areas and control hearts (c). TTC staining of the same infarcted heart confirmed the location of the ischemic injury (d).

the amplitude of the background channel (a_b) assigned to the green component. The fold change (or ratio) of thoracic to hepatic regions was 0.22 ± 0.06 for the CW image (representing a larger liver signal), while it was 3.13 ± 0.46 for the lifetime-unmixed thoracic channel amplitude image (a_{th}), thereby resulting in a greater than 10-fold increase in contrast for separating the thoracic signal.

3.4 *In Situ Imaging Confirms Location of Fluorescence Signal*

From the *in situ* images (Fig. 5), we observed high fluorescent signal from the liver in CW images of both infarcted and control animals. However, the corresponding lifetime images reveal a significant increase in cardiac lifetime from ischemic myocardium (0.72 ± 0.06 ns) when compared with the liver (0.51 ± 0.02 ns, $p < 0.05$) that is not seen in the thoracic regions of control mice. The lifetime from the liver in control animals (0.51 ± 0.03 ns) compared well with that observed in infarcted mice, but the large liver signal made lifetime measurements of the heart impossible.

3.5 *Ex-Vivo Images Demonstrate That Lifetime Increases in Ischemic Myocardium*

There was an increase in CW fluorescence within the infarcted region, resulting in part from increased probe accumulation (Fig. 4). Lifetimes were calculated in both infarcted and remote regions (infarcts were typically confined to the anterolateral wall while the remote area was defined as a region in the septum). The FL results revealed a modest but significant increase in infarct lifetime when compared with remote areas of the myocardium (infarct—0.67 ± 0.04 ns; remote—0.59 ± 0.05 ns; $p < 0.05$). Note that the lifetime measured in the infarct *ex-vivo* and the lifetime measured in the thoracic region *in vivo* (0.70 ± 0.03 ns Fig. 2) are within reasonable levels of uncertainty for lifetime estimation.[14] Substantial heterogeneous probe accumulation was not observed in the control mice that did not undergo surgery (0.59 ± 0.03 ns). TTC staining confirmed that the location of the infarct correlated with the region of increased lifetime.

4 Discussion

Although, previous studies have applied the CW fluorescence approach to image fluorescent probes in the heart,[4,5] a limitation of this approach is the inability to separate probe concentration from lifetime. Both concentration and FL independently affect the measured CW intensity.[6] When imaging activatable probes, this translates to an inability to separate the contribution of probe uptake from that of pure activation, especially for probes where nonradiative quenching, such as fluorescence resonance energy transfer (FRET[6]) or ground state complex formation, is the underlying mechanism. Furthermore, activatable probes, known to be less than 100% quenched in the inactive state, are activated due to enzyme cleavage within the liver.[4] Thus the measured signal is mixed with a large nonspecific signal from surrounding tissue. While previous work has shown that cleavage of FRET pairs can increase lifetime,[3,26] this has not yet been quantified in infarcted myocardium.

The purpose of this study was to determine if lifetime-sensitive detection could be used to improve imaging of protease activation. Using TD imaging, we have observed that the PGC-800 probe used in this study showed a lifetime shift both *in vitro*, due to pancreatic trypsin cleavage, and *in vivo*, due to inflammation in ischemic regions of the myocardium in mice after coronary ligation. This lifetime shift improves the contrast needed to separate thoracic signal from nonspecific background signal, most of which is emitted from the liver. While the CW intensity increase can be attributed to several factors (including probe uptake or concentration and laser excitation intensity), a lifetime increase is a direct indication of probe cleavage due to a decrease in nonradiative quenching upon activation. Indeed, variations in excitation laser intensity and exposure time likely explain the differences in scale of the arbitrary CW fluorescence units between animals, while lifetime values imaging did not vary with these factors. It is noteworthy that trypsin activation increased fluorescent intensity more than 23-fold, but probe lifetime only increased 1.6-fold. Previous publications using activatable probes have also observed a similar difference in lifetime versus intensity ratios.[3] We believe this difference between intensity and lifetime ratios is likely due to the multiple underlying quenching mechanisms.[6,27] The focus of this paper was to demonstrate the use of lifetime contrast as a feasible approach for *in vivo* imaging in the myocardium. Identifying the origin of

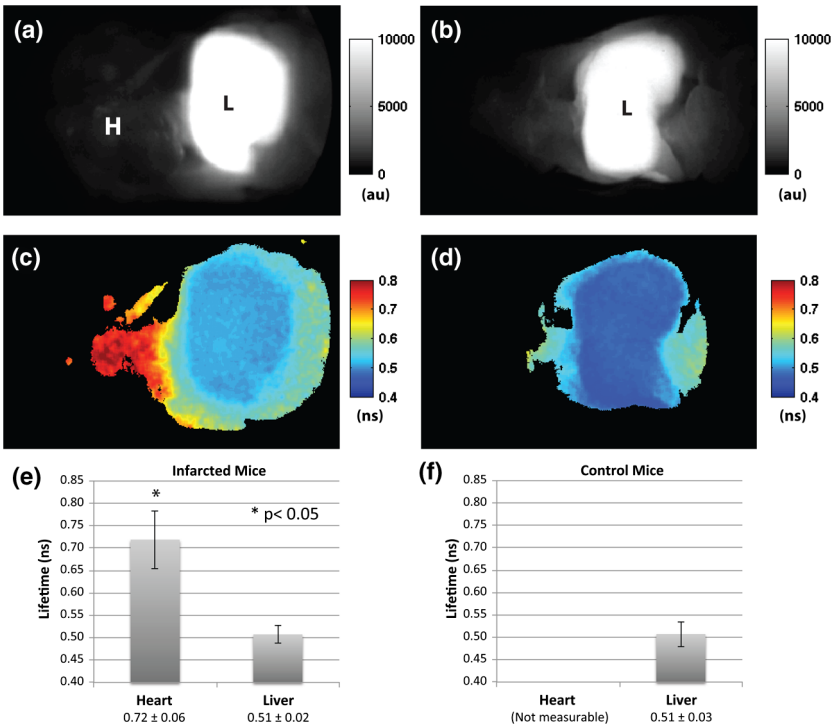

Fig. 5 *In situ* imaging confirmed origin of fluorescence signal. CW images show large liver signal for both infarcted (a) and control mice (b). Lifetime maps confirmed that longer lifetime fluorescence comes only from infarcted myocardium (c) and is not seen in control animals (d). This increase in lifetime (e) from infarcted mice was significant ($p < 0.05$). The *in situ* fluorescent signal from the heart in control mice was not measurable due to the large liver signal, but the liver lifetimes compared well with the measurements from infarcted animals. H = heart, L = liver.

quenching in activatable probes and corresponding changes in lifetime will require careful further study.

Since intramolecular quenching can occur by several mechanisms[6] care must be taken when linking probe activation to an increase in FL.[3] We have also imaged a commercially available cathepsin-activatable probe (ProSense® 750, Perkin Elmer, Inc., Boston, MA) and found that trypsin cleavage does not significantly increase FL. *In vivo* images, however, do reveal a lifetime increase in infarcted myocardium when compared with signal from the liver. Unfortunately, this shift is significantly less than that observed with PGC-800, making the ability to deconvolve multiple lifetime components considerably more difficult. This underscores the importance of developing probes specifically tailored for lifetime imaging.

We have also observed that probe lifetime is influenced by the local environment, as the FL *in vivo* is longer than that measured *in vitro* due to trypsin activation. Specifically, the lifetime of activated PGC-800 due to trypsin was 0.47 ± 0.01 ns but increased to 0.70 ± 0.03 ns and 0.67 ± 0.04 ns when measured in myocardial infarcts from either *in vivo* or *ex-vivo* images, respectively. This observation suggests that, in addition to pure probe activation, local tissue factors also affect FL.[10,28] Previous work has shown that pH[11,29] and the internalization of target-specific activatable antibody-fluorophore conjugates[30] can influence the lifetime of some fluorescent probes. These environmental effects likely influenced the FL measurements reported here, as the heart and liver are very different microenvironments.[31] Separation of the pure activation contribution from environmental effects would require additional measurements of carefully designed control probes with varying distances between 800CW fluorophores. Future work will be needed for further characterization of environmental effects on both *in vivo* and *ex-vivo* lifetime behavior.

The bi-exponential mapping, where two lifetimes were defined *a priori*, clearly separated infarcted myocardial signal from background fluorescence. While this dual "channel" analysis is an appropriate model for *in vivo* images where two lifetime components dominate, a single exponential fit is still needed to determine lifetime values on a pixel-by-pixel basis. This mono-exponential analysis fits the exponential decay curves well for each pixel and was used to determine the best lifetime values for the bi-exponential mapping. The longer thoracic amplitude component a_{th} from the bi-exponential analysis can, in fact, also be directly used in tomography algorithms to further localize activatable fluorophores within a 3-D volume.[8] Tomography could aid in the localization of ischemic regions and may even provide high enough resolution to measure the amount of cardiac inflammation. This would be helpful in future longitudinal studies designed to quantify the myocardial response to ischemia, where significant macrophage infiltration (persisting for seven to 10 days after coronary ligation) follows an initial invasion of neutrophils.[5]

In summary, the results of this study suggest that FL of the cathepsin-activatable probes increases significantly in infarcted myocardial tissue. In addition, lifetime contrast allows fluorescence due to protease activation in the heart to be distinguished from background signal. The increase in the ratio between the thoracic and hepatic regions with the TD analysis suggests that lifetime contrast can significantly improve the imaging of activatable fluorophores in the myocardium. Additional work will be needed to further quantify the lifetime increase due to probe activation and local environment, with the ultimate goal of enhancing 3-D tomographic imaging of the myocardium.

Acknowledgments

This study was supported by NIH Grants R01 HL093038, R01 AG026240, R01 EB015325, and T32 HL076136. We also gratefully acknowledge Soeun Ngoy for his surgical help and Thomas J. Brady, MD, for his support.

References

1. V. Ntziachristos et al., "Looking and listening to light: the evolution of whole-body photonic imaging," *Nat. Biotechnol.* **23**(3), 313–320 (2005).
2. D. E. Sosnovik, M. Nahrendorf, and R. Weissleder, "Targeted imaging of myocardial damage," *Nat. Clin. Pract. Cardiovasc. Med.* **5**(Suppl 2), S63–S70 (2008).
3. M. Solomon et al., "Detection of enzyme activity in orthotopic murine breast cancer by fluorescence lifetime imaging using a fluorescence resonance energy transfer-based molecular probe," *J. Biomed. Opt.* **16**(6), 066019 (2011).
4. D. E. Sosnovik et al., "Fluorescence tomography and magnetic resonance imaging of myocardial macrophage infiltration in infarcted myocardium *in vivo*," *Circulation* **115**(11), 1384–1391 (2007).
5. M. Nahrendorf et al., "Dual channel optical tomographic imaging of leukocyte recruitment and protease activity in the healing myocardial infarct," *Circ. Res.* **100**(8), 1218–1225 (2007).
6. J. R. Lakowicz, *Principles of Fluorescence Spectroscopy*, 2nd Ed., Springer, New York, NY (1999).
7. R. Weissleder et al., "*In vivo* imaging of tumors with protease-activated near-infrared fluorescent probes," *Nat. Biotechnol.* **17**(4), 375–378 (1999).
8. A. T. N. Kumar et al., "A time domain fluorescence tomography system for small animal imaging," *IEEE Trans. Med. Imag.* **27**(8), 1152–1163 (2008).
9. P. I. Bastiaens and A. Squire, "Fluorescence lifetime imaging microscopy: spatial resolution of biochemical processes in the cell," *Trends Cell Biol.* **9**(2), 48–52 (1999).
10. D. J. Hall et al., "*In vivo* simultaneous monitoring of two fluorophores with lifetime contrast using a full-field time domain system," *Appl. Opt.* **48**(10), D74–D78 (2009).
11. M. Y. Berezin et al., "Near-infrared fluorescence lifetime ph-sensitive probes," *Biophys. J.* **100**(8), 2063–2072 (2011).
12. R. J. Goiffon et al., "Dynamic noninvasive monitoring of renal function *in vivo* by fluorescence lifetime imaging," *J. Biomed. Opt.* **14**(2), 020501 (2009).
13. R. E. Nothdurft et al., "*In vivo* fluorescence lifetime tomography," *J. Biomed. Opt.* **14**(2), 024004 (2009).
14. S. B. Raymond et al., "Lifetime-based tomographic multiplexing," *J. Biomed. Opt.* **15**(4), 046011 (2010).
15. D. J. Hall et al., "Dynamic optical imaging of metabolic and NADPH oxidase-derived superoxide in live mouse brain using fluorescence lifetime unmixing," *J. Cereb. Blood Flow Metab.* **32**(1), 23–32 (2011).
16. P. R. Selvin, "The renaissance of fluorescence resonance energy transfer," *Nat. Struct. Biol.* **7**(9), 730–734 (2000).
17. W. Akers et al., "*In vivo* resolution of multiexponential decays of multiple near-infrared molecular probes by fluorescence lifetime-gated whole-body time-resolved diffuse optical imaging," *Mol. Imag.* **6**(4), 237–246 (2007).
18. A. T. N. Kumar et al., "Feasibility of *in vivo* imaging of fluorescent proteins using lifetime contrast," *Opt. Lett.* **34**(13), 2066–2068 (2009).
19. U. Mahmood et al., "Near-infrared optical imaging of protease activity for tumor detection," *Radiology* **213**(3), 866–870 (1999).
20. C. H. Tung et al., "*In vivo* imaging of proteolytic enzyme activity using a novel molecular reporter," *Cancer Res.* **60**(17), 4953–4958 (2000).
21. C. H. Tung et al., "Preparation of a cathepsin d sensitive near-infrared fluorescence probe for imaging," *Bioconjug. Chem.* **10**(5), 892–896 (1999).
22. C. Bremer, C. H. Tung, and R. Weissleder, "*In vivo* molecular target assessment of matrix metalloproteinase inhibition," *Nat. Med.* **7**(6), 743–748 (2001).
23. E. Marecos, R. Weissleder, and A. Bogdanov Jr., "Antibody-mediated versus nontargeted delivery in a human small cell lung carcinoma model," *Bioconjug. Chem.* **9**(2), 184–191 (1998).
24. A. A. Bogdanov, Jr. et al., "A new macromolecule as a contrast agent for MR angiography: preparation, properties and animal studies," *Radiology* **187**(3), 701–706 (1993).
25. L. H. Michael et al., "Myocardial ischemia and reperfusion: a murine model," *Am. J. Physiol.* **269**(6 Pt. 2), H2147–H2154 (1995).
26. A. L. Rusanov et al., "Lifetime imaging of FRET between red fluorescent proteins," *J. Biophoton.* **3**(12), 774–783 (2010).
27. M. Ogawa et al., "H-type dimer formation of fluorophores: a mechanism for activatable, *in vivo* optical molecular imaging," *ACS Chem. Biol.* **4**(7), 535–546 (2009).
28. M. Y. Berezin and S. Achilefu, "Fluorescence lifetime measurements and biological imaging," *Chem. Rev.* **110**(5), 2641–2684 (2010).
29. A. Almutairi et al., "Biodegradable ph-sensing dendritic nanoprobes for near-infrared fluorescence lifetime and intensity imaging," *J. Am. Chem. Soc.* **130**(2), 444–445 (2008).
30. R. Alford et al., "Fluorescence lifetime imaging of activatable target specific molecular probes," *Contrast Media Mol. Imaging* **5**(1), 1–8 (2010).
31. N. N. Malouf et al., "Adult-derived stem cells from the liver become myocytes in the heart *in vivo*," *Am. J. Pathol.* **158**(6), 1929–1935 (2001).